

Performance of hybrid electric vehicle air-conditioning using SiO₂/POE nanolubricant

N.N.M. Zawawi^a, A.H. Hamisa^{b,c}, W.H. Azmi^{a,b,*}, Tri Yuni Hendrawati^d, S. Safril^{b,e}

^a Centre for Research in Advanced Fluid and Processes, Lebuhraya Tun Razak, 26300, Gambang, Kuantan, Pahang, Malaysia

^b Faculty of Mechanical and Automotive Engineering Technology, Universiti Malaysia Pahang Al-Sultan Abdullah, 26600, Pekan, Pahang, Malaysia

^c Faculty of Science, Engineering and Agrotechnology, University College of Yayasan Pahang, 25050, Kuantan, Pahang, Malaysia

^d Department of Chemical Engineering, Universitas Muhammadiyah Jakarta, Jl. Cempaka Putih Tengah 27, Jakarta, 10510, Indonesia

^e Department of Automotive Engineering Technology, Politeknik STMI, Jakarta, Indonesia

ARTICLE INFO

Handling Editor: Huihe Qiu

Keywords:

Nanolubricants
Coefficient of performance
Hybrid electric vehicle
Air-conditioning system
Silicon dioxide

ABSTRACT

The automobile air-conditioning (AAC) system uses the most energy among all auxiliary components in hybrid electric vehicles (HEV) with an electrically-driven compressor (AAC-EDC). Incorporating nanolubricant improves AAC-EDC performance and reduces battery and AAC component size. This study aims to assess the performance of an AAC-EDC system by employing SiO₂/POE nanolubricants. The performance of the AAC-EDC was examined using SiO₂/POE with a volume concentration of up to 0.01 %, a refrigerant charge of 120–160 g, and a compressor speed of 1200–3840 rpm. The performance of the AAC system was measured by its heat absorption, compressor work, coefficient of performance (COP), and EDC power consumption. The SiO₂/POE was stable for 30 days with a zeta potential of 102.5 mV. The SiO₂/POE demonstrated superior performance over the pure POE lubricants. The compressor work and power consumption were reduced to 26.17 % and 11.97 %, respectively. The lowest expansion valve discharge temperature of 9.6 °C was achieved at 160 g refrigerant charge and compressor speed of 3840 rpm. The nanolubricant attained the highest COP of 3.36 at 1860 rpm speed and 160 g charge. The SiO₂/POE nanolubricant with a volume concentration of 0.01 % is highly recommended for optimal performance in the AAC-EDC system.

Nomenclature

AAC	automobile air-conditioning
BDE	belting-driven compressor
COF	coefficient of friction
COP	coefficient of performance
cSt	centistokes
EDC	electrically-driven compressor
EDX	energy dispersive X-ray
FESEM	field emission scanning electron microscopy

* Corresponding author. Centre for Research in Advanced Fluid and Processes, Lebuhraya Tun Razak, 26300, Gambang, Kuantan, Pahang, Malaysia.

E-mail addresses: naal30@gmail.com (N.N.M. Zawawi), hamisa@ucyp.edu.my (A.H. Hamisa), wanzmi2010@gmail.com (W.H. Azmi), yuni.hendrawati@umj.ac.id (T.Y. Hendrawati), safiril@kemenperin.go.id (S. Safril).

<https://doi.org/10.1016/j.csite.2023.103717>

Received 22 August 2023; Received in revised form 10 October 2023; Accepted 2 November 2023

Available online 4 November 2023

2214-157X/© 2023 The Authors. Published by Elsevier Ltd. This is an open access article under the CC BY-NC-ND license (<http://creativecommons.org/licenses/by-nc-nd/4.0/>).

HEV	hybrid electric vehicles
HFC	hydrofluorocarbon
PAG	polyalkylene glycol
POE	polyol-ester
PPE	personal protective equipment
PWM	pulse width modulation
TEM	transmission electron microscopy
VCRS	vapour compression refrigeration system

Symbols

φ	volume concentration, %
h	enthalpy
m	mass, g
μ	dynamic viscosity, cSt
N	Compressor speed, rpm
\dot{Q}_L	cooling capacity, kJ/kg
Q_L	heat absorption, kJ/kg
P	pressure, kPa
P_c	Power consumption, W
ρ	density, kg/m ³
T	temperature, °C
W_{in}	Compressor work, kJ/kg

Subscripts

L	lubricant
p	nanoparticle

1. Introduction

The automotive air-conditioning (AAC) system consumes the most energy among the auxiliary components in the conventional vehicle and hybrid electric vehicle (HEV) [1]. The utilization of additional load by the AAC system reduces efficiency, wastes energy, increases fuel consumption and increases greenhouse gas emissions. Globally, the use of fuel and the efficiency of energy are becoming the most pressing concerns. According to Atik and Aktas [2], the AAC system consumes the most energy among the auxiliary components in the vehicle. The system also is the second largest energy used in cars after the power train [3]. In addition, Rugh et al. [4] concluded that using air conditioning in vehicles strengthens the greenhouse effect. Fontaras et al. [5] have reviewed that fuel consumption associated with the AAC system increased up to 27 %. In another paper, Carlson et al. [6] also stated that the operation of the AAC system is one of the most significant factors affecting real-world fuel consumption. Recent AAC systems employ the vapour compression refrigeration cycle to provide thermal comfort in the vehicle cabin. The air temperature and relative humidity determine thermal comfort in the passenger compartment [7]. The AAC system requires substantial energy and contributes to greenhouse gas emissions to maintain passenger thermal comfort in adverse weather conditions.

An engine powers the air-conditioning system in a conventional vehicle through a belting-driven compressor (BDC). In contrast, the HEV uses an electrically-driven compressor (EDC) to operate the air-conditioning system and is powered by direct current from the vehicle's battery. The AAC-EDC system's power source is a significant concern in HEV. The exclusively available energy for HEV propulsion is the electricity stored in the battery pack, so additional power consumed by the AAC-EDC system will affect the overall performance of the HEV. With the compact design of the AAC system, the need for energy will consume size, weight, space, and the cost of the battery. Appropriate lubricants may enhance the compressor's performance and dependability [8]. The working fluid in the AAC system consists of refrigerant and compressor lubricant. Most lubricant is in the compressor, and some are circulating in the AAC system. The compressor lubricant is used to lubricate the compressor. The EDC is easy to set up and maintain and has a significant potential for lowering fuel usage [9]. By boosting the air conditioning system's efficiency, it is possible to minimize fuel or energy consumption and emissions to obtain the required thermal comfort. These allow the air conditioning system to contribute less to the environmental problem and minimize the rising worldwide demand for energy. The AAC system's lubricant type is the most significant distinction between the EDC and the BDC. Polyalkylene-glycol (PAG) lubricant is primarily used in conventional AAC system while polyol-ester (POE) lubricant is commonly used in AAC-EDC system [10–12].

Many approaches and research have been explored to enhance the performance and improve the AAC system's energy saving [13, 14]. In addition, the performance of the AAC system must be improved to eliminate the environmental effect and reduce the dependence on worldwide fuel usage. The performance and workload of the AAC system can be improved through vapour compression technologies [15–18]. Despite its high energy consumption and poor environmental consequences, the vapour compression refrigeration system (VCRS) is a widespread refrigeration method [18]. One of the passive methods is by introducing nanolubricants in the AAC system [19]. The compressor's performance in the AAC system can be enhanced by integrating the nanoparticles dispersion

technology by introducing nanoparticles into the refrigeration system, namely nanolubricant [20] and nanorefrigerant [21]. The nanolubricant and nanorefrigerant have been employed frequently in VCERS and proven with high potential for improving the system's thermodynamic and mechanical performance. The dispersion of nanoparticles for VCERS can be done in two ways. The first technique for nanorefrigerant involves dispersing nanoparticles into the refrigerant. In contrast, the second method for nanolubricant comprises dispersing nanoparticles into the compressor lubricant and using nanolubricant in the AAC-EDC system to improve overall performance. There are several advantages of using nanolubricant in the AAC system. The nanolubricant can improve the miscibility and solubility of the refrigerant-lubricant mixture, increase thermal properties, and enhance tribological properties [22]. However, the non-conductive compressor lubricant requires proper nanoparticle material selection for dispersing into the POE lubricant.

The changes in heat transfer properties, tribology, and refrigerant mixture characteristics may affect the compressor's and system's pressure characteristics [23]. In one of the findings, it has been shown that various working pressures are used in a vapour compression system, giving different results for the compression work and, thus, the power consumption [24]. Mineral oil with TiO₂ nanoparticles was tested in a residential refrigerator by Bi et al. [25] and is considered one of the pioneering works for nanolubricant in VCERS. R134a refrigerant and POE lubricant were used in their investigation. The refrigerator's performance with nanoparticles was evaluated using energy-saving testing equipment and utilized with 26.1 % less energy. On the other hand, Subramani and Prakash [26] attained up to 25 % energy consumption reduction when they employed Al₂O₃/MO nanolubricants in VCERS. The Al₂O₃/PAG nanolubricant was tested in an AAC-BDC system experiment by Redhwan et al. [27]. In their investigation, the optimal Al₂O₃/PAG nanolubricant with 0.01 % volume concentration offered the maximum performance of the AAC-BDC system. Al₂O₃/PAG nanolubricant, with an average of 28 %, had the most significant COP increase of up to 31 %. Redhwan et al. [28] have studied the thermo-physical characteristics of composite nanolubricant. Al₂O₃ and SiO₂ nanoparticles were dispersed into PAG lubricant to formulate the Al₂O₃-SiO₂/PAG composite nanolubricant. The maximum thermo-physical characteristics of composite nanolubricants have been reported at a volume concentration of 0.1 %, with a rise in thermal conductivity of up to 2.4 % and an increase in viscosity of up to 9.71 %, respectively. Therefore, the use of nanolubricant in VCERS is promising to improve the overall system performance in terms of heat transfer characteristics, tribological performance, and refrigerant-lubricant solubility behaviour [29,30]. However, the investigation on AAC performance with nanolubricant is limited in literature compared to other refrigeration systems performance with nanolubricant. But to the best of the author's knowledge, none research is undertaken for nanolubricant in AAC-EDC system.

Although the performance of the AAC system with nanolubricant has been documented in prior studies, these reports focused mainly on BDC and PAG nanolubricants [31,32]. However, a limited study was undertaken for AAC-EDC with POE lubricant and none with nanolubricants. Therefore, in this study, the influence of nanolubricants on the performance of the AAC system will be investigated. Nanolubricants comprised of SiO₂/POE combination are prepared in a two-step method, and stability investigation was carried out. Then, an AAC system test bench is designed to experimentally examine AAC system performance by utilizing the SiO₂/POE combination. The performance of SiO₂/POE nanolubricant for the AAC-EDC system is investigated. The experimental investigation is then carried out to gather data and support using nanolubricants in the AAC-EDC system.

2. Materials and methods

2.1. Descriptions of nanoparticles and lubricants

Metal oxide nanoparticles, namely SiO₂, were used to prepare nanolubricants. This study used SiO₂ (amorphous) nanoparticles with 99.9 % purity and an average size of 30 nm with a spherical shape. The SiO₂ nanopowder was procured from Beijing DK Nanotechnology. In order to assess the chemical composition of the nanoparticles, EDX analysis was utilized. Fig. 1 depicts the corresponding peaks and details of EDX spectrum values measured in atomic and weight percentages using FESEM. Both elements were identified in the EDX, and the atomic percentages of Silicon (Si) and Oxygen (O) were 74.419 and 25.581, respectively. The additional peak element in the EDX spectrum represents the reference peak for the Carbon element, however insignificant. These nanoparticles also were characterized by the transmission electron microscopy (TEM) technique. The properties of the SiO₂ nanoparticles are depicted in Table 1. Wearing the proper personal protective equipment (PPE) and adhering to all safety precautions are advised by the manufacturers when preparing nanolubricants while handling nanoparticles.

The EDC lubricant used in this experiment was polyol-ester (POE), the working fluid for the AAC-EDC system. The EDCs are powered by high-voltage electric motors housed internally. The electric motor coil and other components interact with the compressor

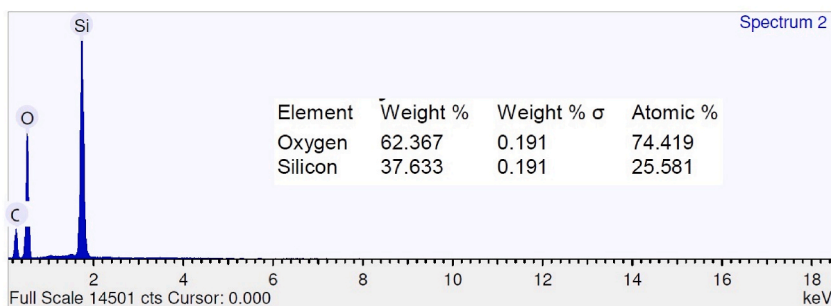


Fig. 1. EDX analysis of the SiO₂ nanoparticles.

Table 1
Properties of SiO₂ nanoparticles [33,34].

Property	Unit	SiO ₂
Thermal Conductivity	W/m.K	1.4
Specific heat	J/k.K	745
Density @ 20 °C	Kg/m ³	2220

oil in these compressors. It must, therefore, possess some degree of electrical short-circuit resistance. Dielectric properties are one factor contributing to the integrity of the electrical windings of a compressor. PAG lubricant is most frequently used in conventional AAC systems, whereas POE (polyol-ester) oil is used most in AAC-EDC systems. The POE is often used in electric compressors in hybrid cars and other cars with electric compressors because it has good dielectric properties and has been used in electric compressors for more than 20 years. This study employed POE RL68H Emkarate, and Table 2 lists the properties of this lubricant. The Emkarate RL 68H, an ISO VG 68 synthetic POE lubricant, is designed for HFC-refrigerant-using compressors for air conditioning and refrigeration systems [35]. This product provides excellent wear protection for steel and aluminium surfaces for longer system life and improved performance. The low-temperature properties and exceptional chemical and thermal stability of POE RL68H allow its application over a broad temperature range. In addition, it is naturally lubricious across a wide temperature range, mixes well with HFCs and other refrigerants, and is chemically stable with other system components.

2.2. Preparation and stability of nanolubricant

$$\varphi = \frac{\frac{m_p}{\rho_p}}{\frac{m_p}{\rho_p} + \frac{m_L}{\rho_L}} \times 100 \quad (1)$$

Determining the mass of the nanoparticles is the first step in preparing the nanolubricant. The specific mass of nanoparticles needed with a high precision weight balance with a resolution of 0.001 g for a predefined volume concentration was determined using Equation (1).

where φ is the volume concentration in percent, m_p and m_L are the lubricant and nanoparticle masses, respectively, with ρ_p and ρ_L are the lubricant and nanoparticle density, respectively. Moreover, to prevent the formation of clumps, each nanoparticle is passed through a filter in addition to being weighed.

All the nanolubricants were prepared using a two-step method, with variations in volume concentration of up to 0.1 %. A magnetic stirrer was used to distribute the nanoparticles throughout the lubricant evenly. The mechanical agitation technique lasted for around 30 min at room temperature. As the process continued, the nanolubricants were stabilized, and the size of the aggregation diminished. Before proceeding with the performance measurement, the nanolubricant must be stabilized and its agglomeration reduced to avoid any impending problems. The nanolubricant was then continuously homogenized while stirring and agitated using a Fisherbrand FB15015 ultrasonic bath vibrator. The ultrasonication process serves several functions, the most important of which are the deagglomeration of nanoparticles, the reduction in nanoparticle size, the production and deposition of nanoparticles, and the distribution of nanoparticles into the base fluids [36]. The ultrasonic bath vibrator homogenizer generates ultrasonic pulses at a frequency of 50 kHz. The bath frequency, water temperature, and volume are constant throughout the sonication process. The nanolubricant was found to be best sonicated for 3 h without the addition of surfactant. Therefore, the samples that had been sonicated for 3 h for the best stability were then fixed throughout the study as the evaluation of the nanolubricants' stability and performance progressed. Fig. 2 demonstrates an illustration of the process of preparing nanolubricants. The current study's stability evaluation methodology includes the sedimentation photographing technique, micrograph evaluation, and zeta potential measurement.

2.3. Experimental setup for AAC-EDC system

An experimental setup known as the AAC test rig was created and developed to test the efficiency of the system while using the new lubricant. In particular, the original components of the AAC system from a hybrid car were used to build this experimental setup, which was constructed using the same materials as the actual car or vehicle. This AAC system was mounted on the test rig setup, including a water bath for an evaporator, an inverter frequency controller, a data logger, and various kinds of piping systems and instruments for measurement. The configuration of the AAC-EDC system test rig is depicted in Fig. 3. The main components of a typical AAC system are the condenser, evaporator, expansion valve, compressor, receiver drier, and piping system. In the current study, the AAC system was designed to use an alternative type of compressor called an electric-driven compressor (EDC). The next crucial component of the AAC

Table 2
Properties of POE RL68H lubricant [35].

Property	Unit	POE RL68H
Viscosity @ 40 °C	cSt	66.6
Viscosity @ 100 °C	cSt	9.4
Pour Point	°C	-39
Density @ 20 °C	g/ml	0.977
Flash Point COC	°C	270

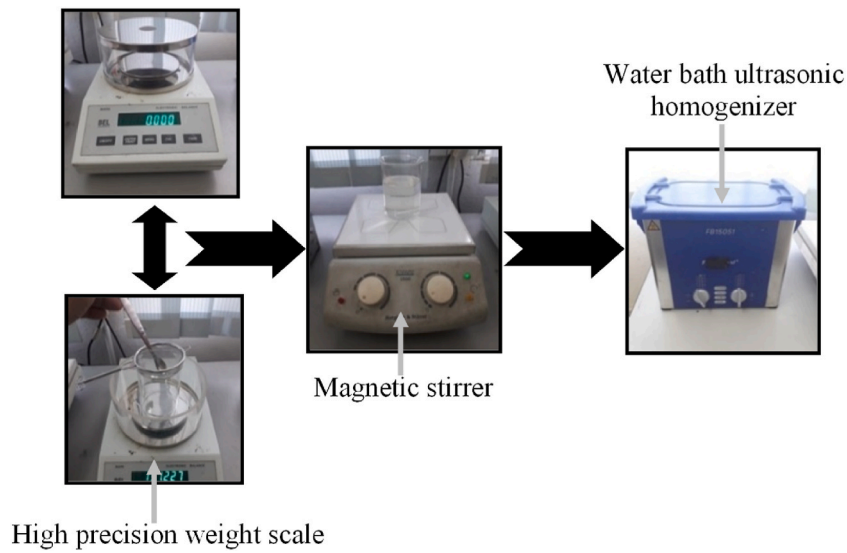


Fig. 2. Process of preparing nanolubricants and instrumentations used.

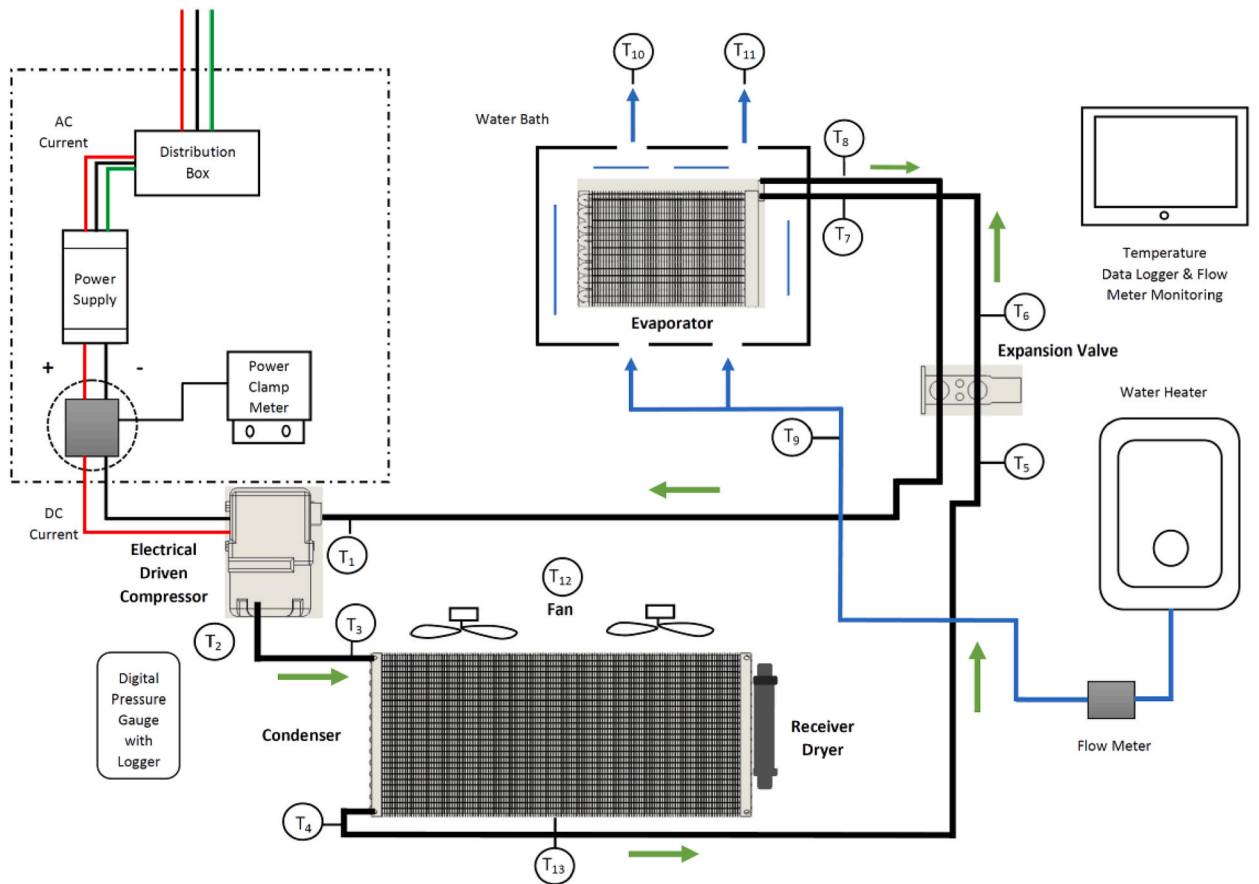


Fig. 3. AAC-EDC system schematic diagram for experimental setup.

system in the study is the driver and control system, which uses electricity to drive the inverter frequency controller and the EDC. The cycling system was installed to prevent the compressor from running continuously throughout the experiment. The third component is the pipe and water bath system for evaporators. This system ensures that the evaporator temperature can be measured quickly and

consistently. The cooling capacity is calculated by immersing the evaporator in a water bath and using the ASHRAE 41.9–2000 calorimeter test procedures for mass flow measurements of volatile refrigerants [37]. The water bath system included a flow transducer, two-way inlet and outlet pipes, a fully insulated tank, and a water heater that managed the water's temperature and flow rate.

The AAC-EDC system was properly instrumented with temperature indicators, pressure gauges, and low-rate sensors. The thermocouple was installed at 12 different locations, including the pipeline for the AAC system and the inlet and outlet points for each major component. A calibrated K-type thermocouple was used to measure the temperatures at these various locations following the ANSI/ASHRAE (1986) standard. The K-type thermocouple, which has a diameter of 0.3 mm and a tolerance of ± 1.5 °C, is designed for temperature ranges between -40 and 375 °C. Each measurement of the water flow rate and temperature measurement was tracked and recorded using a data logger module. The pressures in the evaporator and condenser were measured and recorded using calibrated digital pressure gauges. The power consumption of the AAC-EDC system was manually measured, monitored, and recorded with the assistance of AC/DC power clamps. The test rig was placed in the control room to adhere to the SAEJ2765 [38] standard. The temperature and humidity were maintained between 24.5 and 25.5 °C as well as 45 % and 65 %, respectively.

2.4. Experimental procedures

Each safety procedure and standard must be strictly followed during the development of the AAC-EDC system test rig and once the rig is operational. This procedure ensures that the testing apparatus is always in excellent condition. The equipment, measurement apparatus, sensors, and all other components are inspected to ensure compliance with all security procedures. The AAC-EDC test rig was filled with R134a at a pressure of 300 kPa before the experiment. The pressure was maintained for 24 h to ensure the system was leak-proof. The AAC-EDC system was then evacuated to remove the R134a refrigerant, and nitrogen (N₂) gas was used to ensure that any trapped contaminants had been released. Then, to completely evacuate the AAC-EDC system, a vacuum pump was attached to the service port and operated for one to 2 h. Once the leak test was completed and confirmed that the AAC-EDC system was in good condition, the experimental process to determine its performance was conducted following the rules and recommendations of the SAEJ2765 standard. The parameters of the AAC-EDC system used in the experiment are listed in Table 3.

The EDC was lubricated with 100 ml of POE RL68H lubricant before the commencement of the experiment run. The refrigeration system was then charged with the appropriate amount of R134a. Next, the required refrigerant charge, measured in grams, was determined using a weighing scale. After that, water was added to the bath, completely submerging the evaporator. With the aid of the water heater, the water temperature at the intake and output was balanced. The inlet water flow rate was also sustained at 3 lpm. After completing all pre-experimental procedures, the AAC-EDC system was powered up, and the initial speed was set to 1200 rpm by adjusting the PWM duty cycle. Before that, the frequency was fixed and kept at 50 Hz. After 15 min of operation, the temperature, pressure, power consumption, and water mass flow rate were recorded and logged for 5 min. Afterwards, the data recording was stopped, and the heater and the compressor were turned off.

The experiment was then repeated using various compressor speeds. The compressor speeds varied at 660 rpm intervals between 1200 and 3840 rpm. After completing the initial refrigerant charge, the steps were repeated for subsequent charges of 120–160 g. The procedure was then carried out again for different nanolubricant volume concentrations. The AAC-EDC system must be cleaned by flushing out all the previously used nanolubricants with a refrigerant recovery machine. This step was necessary to ensure that earlier samples did not contaminate the subsequent nanolubricant sample.

2.5. Analysis of performance parameter

After all the data had been gathered and analyzed, the performance parameters of the air conditioning system were established. The POE RL68H lubricant and nanolubricant were used at volume concentrations ranging from 0 to 0.1 %. The specific analytical procedure is therefore described in greater detail in this section. Temperature and pressure sensors concerning compressor work, heat absorption, cooling capacity, and COP are located at specific points and conditions. The exact point of enthalpy value was calculated using the measured temperature and pressure. Then, this experiment used five different initial refrigerant charges, five different volume concentrations, and five different compressor speeds to collect data on temperatures and pressures. This set of data was repeated for nanolubricants. Each data set was repeated three times to ensure its accuracy and dependability.

As recommended by SAE International Standard SAEJ2765 [38], the AAC-EDC was in steady-state conditions before temperature and pressure measurements. The enthalpy at the point of interest was calculated and determined by analyzing the temperature and pressure. Consequently, the heat absorption (Q_L), compressor work (W_{in}), and performance coefficient (COP) can be calculated. The heat absorption, compressor work, COP, cooling capacity (\dot{Q}_L), and EDC power consumption (P_c) are described in Equation (2) to 7, respectively.

$$Q_L = h_1 - h_6 \quad (2)$$

where $h_5 = h_6$.

Table 3
Experimental parameters for the AAC-EDC system.

Parameters	Unit	Range
EDC compressor speed	rpm	1200–3840
Refrigerant charge	Gram (g)	120–160
Volume concentration, φ	%	0–0.01

$$W_{in} = h_2 - h_1 \quad (3)$$

$$COP = \frac{Q_L}{W_{in}} = \frac{h_1 - h_6}{h_2 - h_1} \quad (4)$$

$$\dot{Q}_L = Q_{water} C_{p,water} \Delta T \quad (5)$$

$$\Delta T = T_9 - \left(\frac{T_{10} - T_{11}}{2} \right) \quad (6)$$

$$P_c = IV \quad (7)$$

2.6. Uncertainty analysis

The experiment used measuring devices and sensors such as thermocouples, refrigerant gauges, flow meters, and weighing scales. The list of sensors, apparatus and the degree of accuracy for each instrument is presented in Table 4, and the summary associated with the uncertainty analysis of measured variables and calculated experimental parameters is provided in Table 5 and Table 6, respectively. In the present uncertainty analysis, the variables from measurement are temperature, pressure, power consumption and water flow rate. In contrast, the calculated experimental parameters are heat absorption, cooling capacity, compressor work and coefficient of performance. A fractional uncertainty formula was used to calculate the uncertainties of the present variables. Measured variables had an uncertainty range between 0.01 % and 0.82 %, while calculated experimental parameters had an uncertainty of less than 1 %.

3. Results and discussion

3.1. Stability evaluations of SiO₂/POE nanolubricants

A set of nanolubricants, namely SiO₂/POE, was set aside and kept stationary in test tubes at different volume concentrations. The nanolubricants were kept uninterrupted in the test tubes for up to 30 days to get a precise image. The samples were observed daily. All samples' images were captured on the first day of preparation and again after 30 days for qualitative comparison evaluation. The samples of the nanolubricants at different volume concentrations are shown in Fig. 4. The SiO₂/POE nanolubricants were observed with good stability conditions. However, the transparent physical appearance of SiO₂ nanoparticles in POE lubricants may be hidden in the actual sedimentation condition of this type of nanolubricants. In the present study, it should be noted that no surfactant was utilized to prepare these nanolubricants. This condition is essential to avoid drawbacks to the AAC-EDC system during operation and application. Generally, all samples in the present study were observed with insignificant sedimentation without any visible separation layer between the nanoparticles and lubricants.

The TEM image of SiO₂ nanoparticles suspended in POE RL68H lubricant for amplifications of $\times 180,000$ is shown in Fig. 5. In this type nanolubricants, the micrograph images display the least amount of clustering and aggregation of nanoparticles. The size of SiO₂ nanoparticles is 15 nm, with the nanoparticles observed to be spherical. For nanolubricants, minimal clustering and agglomeration of nanoparticles were observed with good dissemination of nanoparticles in the POE RL68H-based lubricant. The zeta potentials for SiO₂/POE nanolubricants were measured at 102.5 mV. The absolute value of zeta potential above 60 mV is desirable for excellent stability conditions of the nanolubricants. The nanolubricants of this study in Fig. 6 exhibited zeta potential values of more than 60 mV, which is proven to be beyond the stability limit. Therefore, the nanolubricants in this study were confirmed in excellent colloidal condition. Accordingly, the nanolubricants of the present study are concluded to have excellent stability conditions, which can be proceeded for performance evaluations. The nanolubricants' stability is evaluated by comparing the result of the measurement of the absolute value of the zeta potential to the classification of the nanolubricants' stability provided by Lee et al. [39].

3.2. Performance of AAC-EDC using SiO₂/POE nanolubricant

The performance of the AAC-EDC system will be discussed thoroughly in this section and onwards. The section presents the compressor, cooling, and overall system performance outcome. The compressor performance mainly focuses on compressor work and EDC power consumption. In comparison, the cooling performance highlights the heat absorption and cooling capacity of the AAC-EDC system. Lastly, the expansion valve discharge temperature and coefficient of performance (COP) are evaluated to analyze the overall system performance. Initially, the condition and validity of the present AAC-EDC system test rig must be tested thoroughly using POE lubricants before the performance of the nanolubricants can be evaluated. The general trend performance for the AAC-EDC system was determined and compared with previous research works in the literature. The performance of the AAC-EDC system using POE

Table 4
Measuring instrument ranges and accuracy.

Sensors/Equipment	Range	Accuracy
K-type Thermocouple, °C	-40 to 375	±1.5
Refrigerant gauge, kPa	-100 to 6000	±0.5
Water flow meter, LPM	0 to 100	±1.0
Weighing scale, kg	0 to 25	±0.001
Power clamp, kW	1 to 10	±0.01

Table 5
Summary of the uncertainty for the measured variables.

Measured variables	Measurement		Least division in instrument	Uncertainty (%)	
	Min	Max		Min	Max
Pressure, P [kPa]	347	690	± 0.5	0.07	0.14
Temperature, T [$^{\circ}\text{C}$]	12.2	49.5	± 0.1	0.23	0.82
Power consumption [kW]	113.7	175.5	± 0.01	0.01	0.01
Water flowrate, \dot{m} [L/min]	4	4	± 1.0	0.25	0.25

Table 6
Summary of the uncertainty for the calculated experimental parameters.

Calculated variables	Uncertainty (%)
Heat absorption	0.56–0.88
Compressor Work	0.37–0.43
Coefficient of Performance (COP)	0.68–1.00
Cooling Capacity	0.62–0.93

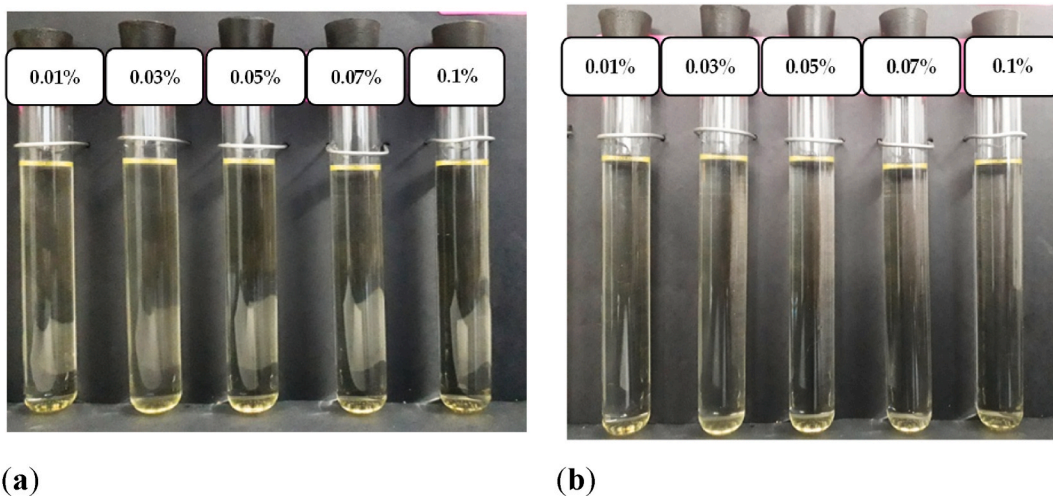


Fig. 4. Visual sedimentation for SiO_2/POE nanolubricants: (a) First day after preparation; (b) After 30 days of preparation.

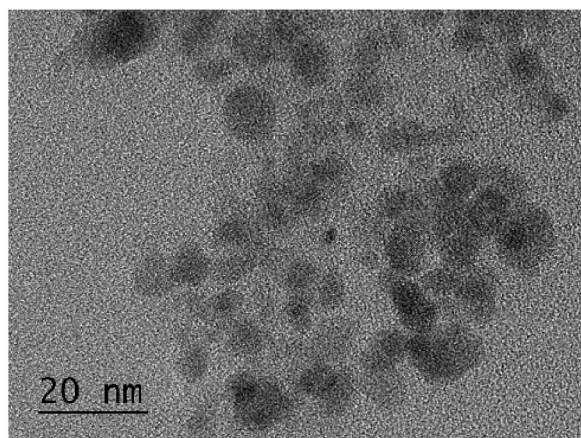


Fig. 5. SiO_2/POE nanolubricants ($\times 180,000$).

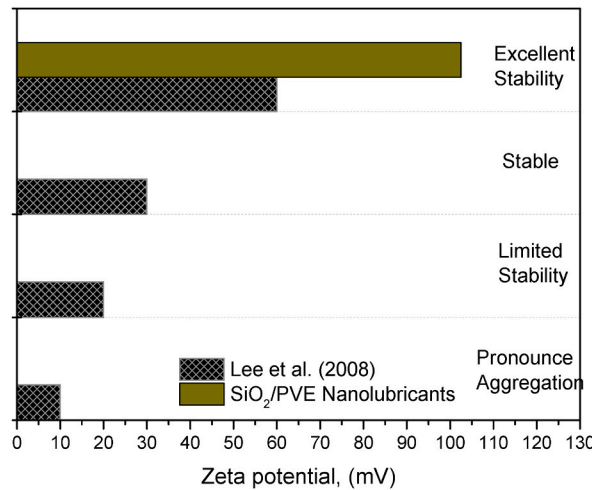


Fig. 6. Zeta potential of SiO₂/POE nanolubricants.

lubricants was used as a baseline for the relative performance evaluation of SiO₂/POE nanolubricants. Initially, the optimal amount of initial refrigerant charge into the AAC-EDC system must be sought to reach the system’s optimum performance and efficiency [27,40,41]. Subsequently, the performance analysis in the present study was evaluated by varying the initial refrigerant charge.

The AAC-EDC system was charged with R134a refrigerant with an initial refrigerant charge between 120 and 160 g to commence the AAC-EDC system operation and verification. Then, the performance of the AAC-EDC system using pure POE lubricants and SiO₂/POE nanolubricant was investigated. The compressor, cooling, and overall system performance were analyzed and plotted against various refrigerant charges. Later, the optimum initial refrigerant charge was determined. The optimum refrigerant charge was confirmed through the expansion valve discharge temperature analysis. The expansion valve discharge temperature, which gives the lowest temperature reading, determines the optimum refrigerant charge.

Fig. 7 portrays the compressor work, W_{in} for SiO₂/POE nanolubricant at 0.01 % volume concentration compared with pure POE lubricants at different compressor speeds and variation of initial refrigerant charge for 120, 140 and 160 g. From the graph, the compressor work of SiO₂/POE nanolubricant increases with increasing the compressor speed and agrees with the trend of pure POE lubricants. These results could be related to the increase in compressor stroke with rising compressor rotation and the amount of initial refrigerant charge [42,43]. Compared to the AAC-EDC system employing pure POE lubricants, the SiO₂/POE nanolubricant in Fig. 7 is considerably lower compressor work than POE lubricants for all refrigerant charges and compressor speeds. Reducing the coefficient of friction (COF) in the compressor is crucial in lowering the compressor’s energy consumption [44]. Therefore, reducing compressor work by SiO₂/POE nanolubricant also contributes to improve tribological performance with lower COF than POE lubricants to deliver smoother and lesser work by the compressor. Other researchers also support this behaviour [27,45,46] in the literature.

Fig. 8 shows the electrically-driven compressor (EDC) power consumption for 0.01 % volume concentration of SiO₂/POE nanolubricant compared to POE lubricants at different compressor speeds and various initial refrigerant charges. The EDC power

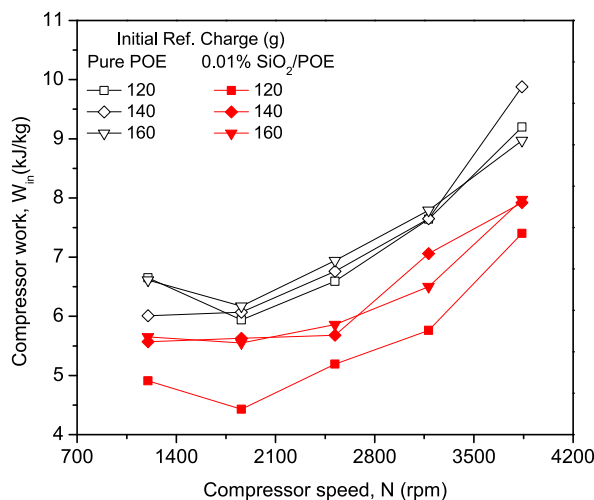


Fig. 7. Compressor work of SiO₂/POE nanolubricant at different compressor speeds.

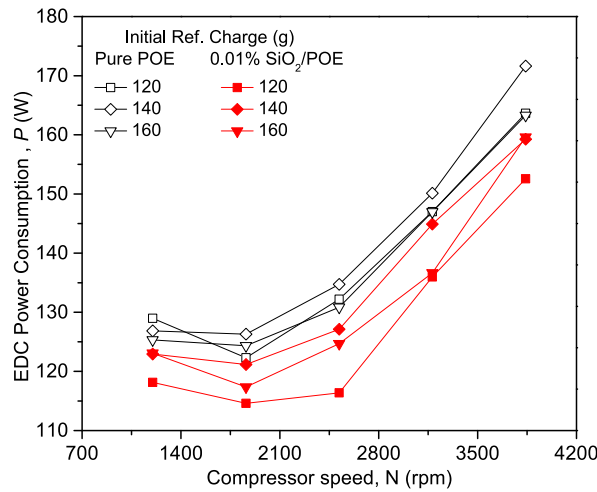


Fig. 8. EDC power consumption of SiO₂/POE nanolubricant at different compressor speeds.

consumption for SiO₂/POE nanolubricant in Fig. 8 increased obviously with the compressor speed. A slight decrement happened at the speed of less than 1840 rpm, but the power consumption was increased back until the maximum speed. This trend was also supported by Atik and Aktas [2] with similar findings in their work. Excitingly, the SiO₂/POE nanolubricant at 0.01 % volume concentration was performed with lower EDC power consumption than pure POE lubricants and followed for all compressor speeds and initial refrigerant charges. The SiO₂/POE nanolubricant using 120 g refrigerant charge at 2520 rpm performed with the highest power consumption reduction compared to the pure POE lubricants. Furthermore, compared to pure POE lubricants, the EDC power consumption decrement also occurred for other refrigerant charges and compressor speeds with smaller drops. This trend agrees with the finding of compressor work reduction in Fig. 7. This result demonstrates that improved tribological performance reduced the compressor work of SiO₂/POE nanolubricant consequently minimizing the compressor’s EDC power consumption. This finding confirmed the feasibility of SiO₂/POE nanolubricant for application in the AAC-EDC system.

The ability to absorb heat by the evaporator, Q_L and the effective expansion valve discharge temperature are considered essential parameters for the cooling performance evaluation of the AAC-EDC system. Fig. 9 represents the heat absorption at different compressor speeds with a variation of initial refrigerant charge for the AAC-EDC system using SiO₂/POE nanolubricants, respectively. In general, from the graph, the heat absorption for nanolubricants increased with the compressor speed and initial refrigerant charge. This trend occurred for SiO₂/POE nanolubricants. A similar pattern was also applied to the previous trend by POE lubricants. From Fig. 9, the SiO₂/POE nanolubricant at 0.01 % volume concentration showed significantly higher evaporator heat absorption than the AAC-EDC system using pure POE lubricants.

The figure confirmed that the evaporator’s heat absorption for the AAC-EDC system with nanolubricants performed better than the pure POE lubricants. This outcome is possibly due to the thermal properties of the nanolubricants. According to Sharif et al. [47], it was observed that the thermal conductivity of low-concentration nanolubricants exhibited a notable increase in comparison to base

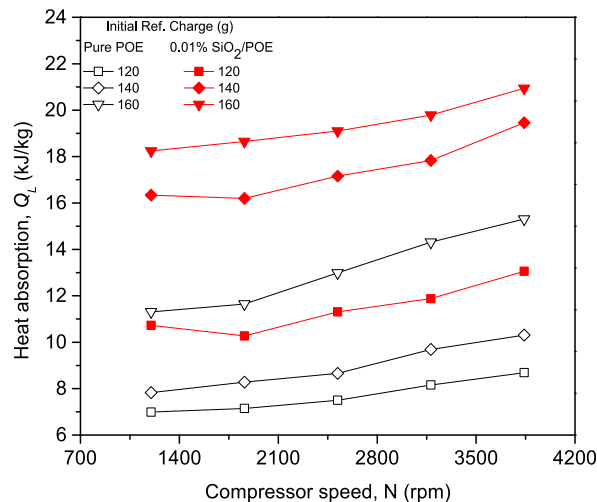


Fig. 9. Heat absorption of SiO₂/POE nanolubricant at different compressor speeds.

lubricants. This enhancement can be attributed to the Brownian motion of nanoparticles within the nanolubricants. Furthermore, incorporating nanoparticles can potentially enhance the lubricant's thermal resistance properties. However, the thermal resistance of nanolubricant is increased because of the grouping of nanoparticles, leading to a decrease in thermal conductivity when aggregation occurs [48]. The thermal resistance between nanoparticles significantly increases as the particle contact radius decreases. The interparticle resistance is notably influenced by the forces acting between particles, precisely the existence or absence of chemical bonds among nanoparticles [49]. Furthermore, as the nanoparticle's diameter decreases, the impact of interfacial force strength on thermal resistance becomes more pronounced. In another paper, Sharif et al. [41] concluded that the performance of the AAC system using SiO₂/PAG nanolubricants was enhanced because of the heat absorption improvement better than base PAG lubricants.

The expansion valve discharge temperature for 0.01 % volume concentration of SiO₂/POE nanolubricant as the function of compressor speed with several initial refrigerant charges is depicted in Fig. 10. The discharge temperature of the nanolubricants was compared to pure POE lubricants in the figure. From the graph, the expansion valve discharge temperature decreased to a particular value by increasing the compressor speed and the initial refrigerant charge. The lowest expansion valve discharge temperature of 9.6 °C was achieved at 160 g initial refrigerant charge and a maximum compressor speed of 3840 rpm. The expansion valve discharge temperature of SiO₂/POE nanolubricant was reduced dramatically compared to pure POE lubricants and complied with all operating conditions. The improvement of lower discharge temperature for SiO₂/POE nanolubricant was attained because the synergies between the compressor performance and the cooling performance were outperformed in the previous section.

Subsequently, the COP variation at different compressor speeds and various initial refrigerant charges was plotted in Fig. 11 for SiO₂/POE nanolubricant at 0.01 % volume concentration. The COP of the SiO₂/POE nanolubricant was compared to pure POE lubricants. Generally, the COP for pure POE lubricants and SiO₂/POE nanolubricant was increased with the initial refrigerant charge. However, it was decreased by increasing the compressor speed. As stated in the previous section, heat absorption and compressor work contributed to this circumstance. Excitingly, the COP of SiO₂/POE nanolubricant at 0.01 % volume concentration was improved remarkably higher than pure POE lubricants for all initial refrigerant charges and compressor speeds. The SiO₂/POE nanolubricant attained the highest COP of 3.36 at 1860 rpm compressor speed and 160 g initial refrigerant charge. In addition, the figure shows a substantial value of COP difference between SiO₂/POE nanolubricant and pure POE lubricants. Therefore, applying SiO₂/POE nanolubricant at 0.01 % volume concentration in the AAC-EDC system performs excellently compared to the original POE lubricants.

3.3. Performance at different volume concentrations

Fig. 12 displays the compressor work for SiO₂/POE nanolubricant at different volume concentrations. The AAC-EDC system using SiO₂/POE nanolubricant was performed with lower compressor work than POE lubricants. The compressor work reduction occurred for almost all volume concentrations except 0.1 % and dropped up to 11.1 % at 0.01 % volume concentration. The compressor work of SiO₂/POE nanolubricant at 0.1 % volume concentration showed a small increment higher than POE lubricants but insignificant. This finding can be related to tribology performance and rheological behaviour. According to the previous literature [27,45,46], the lower COF of nanolubricants than their base lubricants contributes to reducing compressor work by SiO₂/POE nanolubricant in the present study. The compressor with nanolubricants can operate under a low power load, reducing the compressor work significantly. However, the compressor work will increase by increasing the volume concentration of nanolubricants due to the rheological behaviour. The viscosity of nanolubricants was increased with increasing volume concentration [28,47]. Subsequently, the compressor work of SiO₂/POE nanolubricant is higher than POE lubricants at a volume concentration of more than 0.07 % because of a significant viscosity increment.

Fig. 13 depicts the heat absorption for SiO₂/POE nanolubricant at various volume concentrations. From the figure, it was observed that the SiO₂/POE nanolubricant at all volume concentrations absorbed more heat significantly higher than pure POE lubricants with the increment from 33.1 % and up to 44.0 %. The variation of the heat absorption is almost similar for different volume concentrations. The SiO₂/POE nanolubricant's heat absorption fluctuated in a small range between 20.38 and 22.05 kJ/kg, higher than POE lubricants with a heat absorption of 15.31 kJ/kg. Therefore, the present nanolubricant in the AAC-EDC system executes with significant heat absorption improvement higher than POE lubricants for all volume concentrations. However, the variation of the initial refrigerant charge must influence the best heat absorption performance. Even though the SiO₂/POE nanolubricant performs well with heat absorption, the compressor work performance must be scrutinized. It is pointless to claim that the present nanolubricants achieve good performance according to the heat absorption alone if the work done by the compressor is higher than pure POE lubricant at high volume concentration. Therefore, COP analysis is required to conclude the present SiO₂/POE nanolubricants' overall performance by considering both components of compressor work and heat absorption.

After completing the compressor and cooling performance evaluations, further analysis of the coefficient of performance (COP) for the SiO₂/POE nanolubricants was undertaken. Subsequently, Fig. 14 portrays the COP variation for SiO₂/POE nanolubricant at different volume concentrations. From the graph, the COP of SiO₂/POE nanolubricants was confirmed to always be better than POE lubricants for all ranges of volume concentration in the present study. As shown in Fig. 14, the COP enhancement was accomplished by SiO₂/POE nanolubricant at all volume concentrations compared to POE lubricants. The highest COP increment was attained up to 53.8 % by SiO₂/POE nanolubricant at 0.01 % volume concentration. Therefore, the present nanolubricants improved the performance of COP expressively and showed a feasible potential for application in the AAC-EDC system.

The optimum performance of the AAC-EDC system with SiO₂/POE nanolubricants was investigated with varying volume concentrations to obtain the optimum system performance. Table 7 summarises the average enhancement of AAC-EDC system parameters at various volume concentrations. The SiO₂/POE nanolubricants at a volume concentration of 0.01 % exhibit the most significant average decrease in compressor work and the best average increase in the COP. Interestingly, 0.07 % SiO₂/POE nanolubricants indicate the most remarkable heat absorption enhancement of up to 44.0 %. Meanwhile, the heat absorption of 0.01 % is increased to

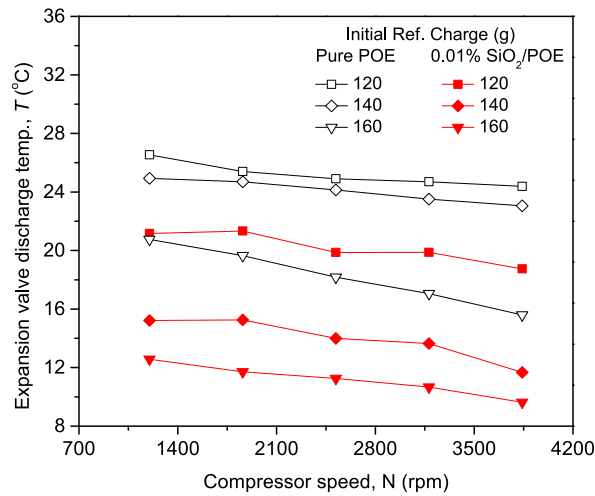


Fig. 10. Expansion valve discharge temperature of SiO₂/POE nanolubricant at different compressor speeds.

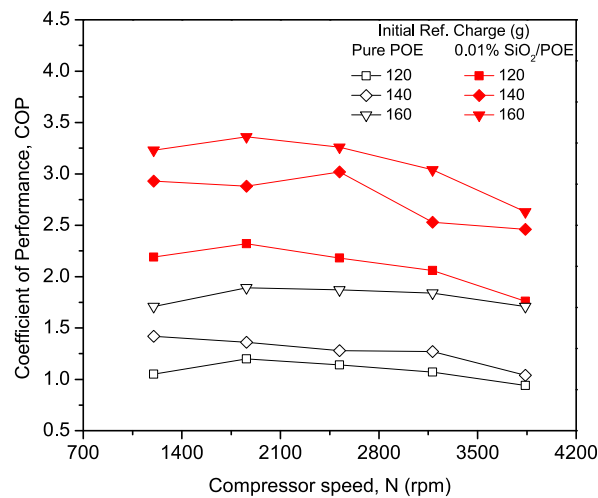


Fig. 11. Coefficient of performance of SiO₂/POE nanolubricant at different compressor speeds.

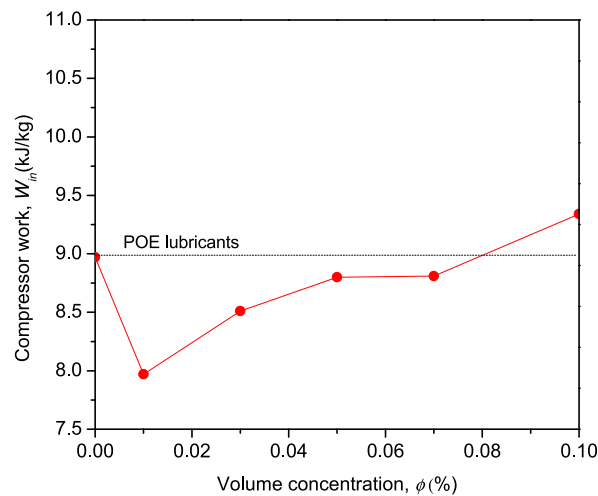


Fig. 12. Compressor work of SiO₂/POE nanolubricant at different volume concentrations.

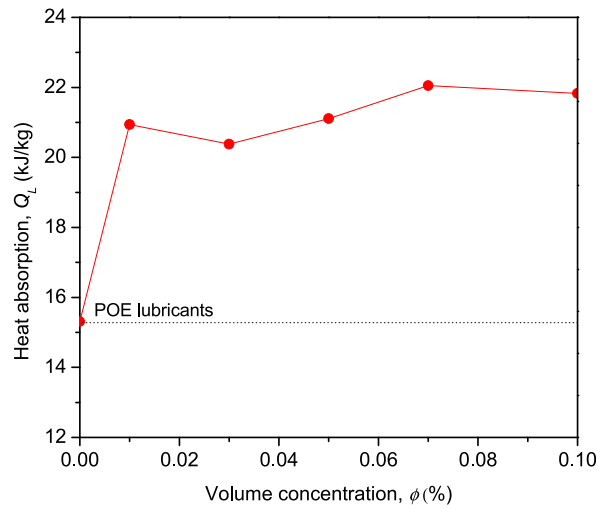


Fig. 13. Heat absorption of SiO₂/POE nanolubricant at different volume concentrations.

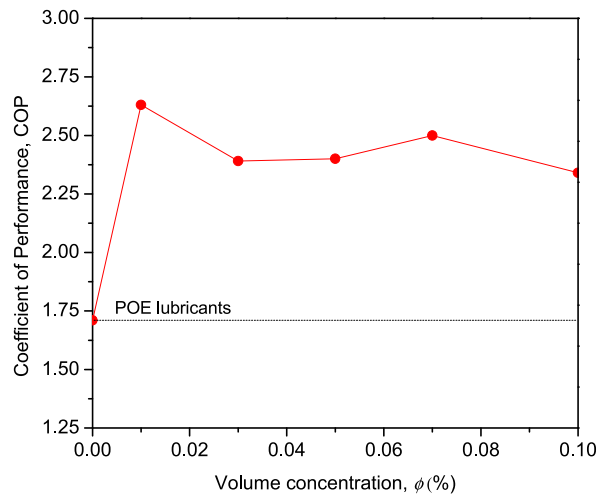


Fig. 14. Coefficient of performance of SiO₂/POE nanolubricants at different volume concentrations.

Table 7

Average enhancement for AAC-EDC system performance with a variation of volume concentrations.

Volume concentration, ϕ (%)	Average enhancement (%)		
	Win (kJ/kg)	QL (kJ/kg)	COP
0.01	-11.1	36.8	53.8
0.03	-5.1	33.1	39.8
0.05	-1.9	37.9	40.4
0.07	-1.8	44.0	46.2
0.10	4.1	42.6	36.8

36.8 %. Finally, the overall performance for the AAC-EDC system seen at 0.01 % volume concentration is deemed satisfactory and improved significantly compared to pure POE lubricants, which exhibit COP improvements for up to 53.8 %.

4. Conclusions

A comprehensive analysis of the performance of the automotive air-conditioning with an electrically-driven compressor (AAC-EDC) system using SiO₂/POE nanolubricant was undertaken. The nanolubricant was prepared using a two-step method, and their stability was evaluated. In addition, the design and development of the test rig were elaborated. The experimental work then

considered heat absorption, compressor work, cooling capacity, coefficient of performance (COP), and EDC power consumption to determine the performance of the AAC-EDC system utilizing nanolubricants. The relationship between heat absorption, compressor work, cooling capacity, coefficient of performance (COP), and EDC power consumption was plotted and discussed. With zeta potential values greater than 60 mV, the SiO₂/POE nanolubricant exhibited the best stability conditions based on visual observation and was found to be in excellent stability conditions. Compared to POE lubricants, the SiO₂/POE nanolubricant with a volume concentration of 0.01 % provides the lowest compressor work and EDC power consumption. Work and energy consumption of the compressor were reduced by a maximum of 26.17 % and 11.97 %, respectively. At 160 g refrigerant charge and 3840 rpm compressor speed, the lowest expansion valve discharge temperature of 9.6 °C was achieved. The SiO₂/POE nanolubricant with a volume concentration of 0.01 % achieved the highest COP increase of up to 53.8 %. The highest COP of 3.36 was performed at a compressor speed of 1860 rpm and a refrigerant charge of 160 g. Therefore, the optimal performance of an AAC-EDC system operating with SiO₂/POE nanolubricants in experimental evaluation is proposed with a volume concentration of 0.01 %. For optimal performance in the AAC-EDC system, it was recommended to use SiO₂/POE nanolubricants with a volume concentration of 0.01 %.

Author statement

We wish to confirm that there are no known conflicts of interest associated with this publication, and there has been no significant financial support for this work that could have influenced its outcome.

We confirm that the manuscript has been read and approved by all named authors and that there are no other persons who satisfied the criteria for authorship but are not listed. We

further, confirm that all have approved the order of authors listed in the manuscript.

We confirm that we have given due consideration to the protection of intellectual property associated with this work and that there are no impediments to publication, including the timing of publication, concerning intellectual property. In so doing, we confirm that we have followed the regulations of our institutions concerning intellectual property.

We understand that the Corresponding Author is the sole contact and represents us for the Editorial process (including the Editorial Manager and direct communications with the office). He is responsible for communicating with the other authors about progress, submissions of revisions and final approval of proofs. We confirm that we have provided a current, correct email address which is accessible by the Corresponding Author and which has been configured to accept email from wanzmi2010@gmail.com.

Declaration of competing interest

The authors declare that they have no known competing financial interests or personal relationships that could have appeared to influence the work reported in this paper.

Data availability

No data was used for the research described in the article.

Acknowledgement

The authors appreciate the financial support provided by the Universiti Malaysia Pahang Al-Sultan Abdullah (RDU222701) and Universitas Muhammadiyah Jakarta (UIC221513) under the International Matching Grant. The authors further acknowledge the contributions of the research teams from the Center for Research in Advanced Fluid and Processes (Pusat Bendalir) and the Advanced Automotive Liquids Laboratory (AALL), who provided valuable insight and expertise for the current study.

References

- [1] G.E. Khoury, D. Clodic, Method of test and measurements of fuel consumption due to air conditioning operation on the new prius II hybrid vehicle, *J. Passeng. Car* 114 (2005) 2563–2571.
- [2] K. Atik, A. Aktas, An experimental investigation of the effect of refrigerant charge level on an automotive air conditioning system, *J. Therm. Sci. Technol.* 31 (2011) 11–17.
- [3] M.A. Roscher, W. Leidholdt, J. Trepte, High efficiency energy management in BEV applications, *Int. J. Electr. Power Energy Syst.* 37 (2012) 126–130.
- [4] J.P. Rugh, T.J. Hendricks, K. Koram, Effect of solar reflective glazing on Ford Explorer climate control, fuel economy, and emissions, in: *Proceedings of the International Body Engineering Conference.*, Vol. Paper Presented at the SAE Technical Paper, 2001.
- [5] G. Fontaras, N.-G. Zacharof, B. Ciuffo, Fuel consumption and CO₂ emissions from passenger cars in Europe—Laboratory versus real-world emissions, *Prog. Energy Combust. Sci.* 60 (2017) 97–131.
- [6] R.B. Carlson, J. Wishart, K. Stutenberg, On-road and dynamometer evaluation of vehicle auxiliary loads, *SAE Int. J. Fuels Lubr.* 9 (2016) 260–268.
- [7] Z. Zhang, J. Wang, X. Feng, L. Chang, Y. Chen, X. Wang, The solutions to electric vehicle air conditioning systems: a review, *Renew. Sustain. Energy Rev.* 91 (2018) 443–463.
- [8] M. Xing, R. Wang, J. Yu, Application of fullerene C60 nano-oil for performance enhancement of domestic refrigerator compressors, *Int. J. Refrig.* 40 (2014) 398–403.
- [9] S.I. Kim, G.H. Lee, J.J. Lee, J.P. Hong, Simple design approach for improving characteristics of interior permanent magnet synchronous motors for electric air-conditioner systems in HEV, *Int. J. Automot. Technol.* 11 (2010) 277–282.
- [10] E.E. Nunez, N.G. Demas, K. Polychronopoulou, A.A. Polycarpou, Tribological study comparing PAG and POE lubricants used in air-conditioning compressors under the presence of CO₂, *Tribol. Trans.* 51 (2008) 790–797.
- [11] S.S. Sanukrishna, M.J. Prakash, Experimental studies on thermal and rheological behaviour of TiO₂-PAG nanolubricant for refrigeration system, *Int. J. Refrig.* 86 (2018) 356–372.
- [12] N.N.M. Zawawi, W.H. Azmi, M.F. Ghazali, Tribological performance of Al₂O₃-SiO₂/PAG composite nanolubricants for application in air-conditioning compressor, *Wear* (2022) 492–493.

- [13] O.A. Alawi, N.A.C. Sidik, M.H. Beriache, Applications of nanorefrigerant and nanolubricants in refrigeration, air-conditioning and heat pump systems: a review, *Int. Commun. Heat Mass Tran.* 68 (2015) 91–97.
- [14] D. Di Battista, R. Cipollone, High efficiency air conditioning model based analysis for the automotive sector, *Int. J. Refrig.* 64 (2016) 108–122.
- [15] C. Park, H. Lee, Y. Hwang, R. Radermacher, Recent advances in vapor compression cycle technologies, *Int. J. Refrig.* 60 (2015) 118–134.
- [16] M.F. Sukri, M.N. Musa, M.Y. Senawi, H. Nasution, Achieving a better energy-efficient automotive air-conditioning system: a review of potential technologies and strategies for vapor compression refrigeration cycle, *Energy* 8 (2015) 1201–1229.
- [17] R.K. Sabareesh, N. Gobinath, V. Sajith, S. Das, C.B. Sobhan, Application of TiO₂ nanoparticles as a lubricant-additive for vapor compression refrigeration systems – an experimental investigation, *Int. J. Refrig.* 35 (2012) 1989–1996.
- [18] M. Bencrta, M. Alshatewi, H. Omar, Developments of vapor-compression systems for vehicle air-conditioning: a review, *Adv. Mech. Eng.* 9 (2017) 1–15.
- [19] N.N.M. Zawawi, W.H. Azmi, M.Z. Sharif, G. Najafi, Experimental investigation on stability and thermo-physical properties of Al₂O₃-SiO₂/PAG nanolubricants with different nanoparticle ratios, *J. Therm. Anal. Calorimetry* 135 (2019) 1243–1255.
- [20] N.N.M. Zawawi, W.H. Azmi, M.F. Ghazali, H.M. Ali, Performance of air-conditioning system with different nanoparticle composition ratio of hybrid nanolubricant, *Micromachines* 13 (2022).
- [21] M.R.M. Nawi, M.Z.A. Rehimi, W.H. Azmi, S.A. Razak, The characterization and thermo-physical property investigations of SiO₂/HFE7000 nanorefrigerants, *Int. J. Refrig.* 88 (2018) 275–283.
- [22] M.Z. Sharif, W.H. Azmi, M.F. Ghazali, N.N.M. Zawawi, H.M. Ali, Numerical and thermo-energy analysis of cycling in automotive air-conditioning operating with hybrid nanolubricants and R1234yf, *Numer. Heat Tran. Part A: Applications* 83 (2023) 935–957.
- [23] M.Z. Sharif, W.H. Azmi, M.F. Ghazali, N.N.M. Zawawi, H.M. Ali, Viscosity and friction reduction of double-end-capped polyalkylene glycol nanolubricants for eco-friendly refrigerant, *Lubricants* 11 (2023).
- [24] R. Cabello, D. Sánchez, R. Llopis, I. Arauzo, E. Torrella, Experimental comparison between R152a and R134a working in a refrigeration facility equipped with a hermetic compressor, *Int. J. Refrig.* 60 (2015) 92–105.
- [25] S. Bi, L. Shi, L.L. Zhang, Application of nanoparticles in domestic refrigerators, *Appl. Therm. Eng.* 28 (2008) 1834–1843.
- [26] N. Subramani, M.J. Prakash, Experimental studies on a vapour compression system using nanorefrigerants, *Int. J. Eng. Sci. Technol.* 3 (2011) 95–102.
- [27] A.A.M. Redhwan, W.H. Azmi, M.Z. Sharif, R. Mamat, M. Samykan, G. Najafi, Performance improvement in mobile air conditioning system using Al₂O₃/PAG nanolubricant, *J. Therm. Anal. Calorimetry* 135 (2019) 1299–1310.
- [28] A.A.M. Redhwan, W.H. Azmi, M.Z. Sharif, R. Mamat, N.N.M. Zawawi, Comparative study of thermo-physical properties of SiO₂ and Al₂O₃ nanoparticles dispersed in PAG lubricant, *Appl. Therm. Eng.* 116 (2017) 823–832.
- [29] N.N.M. Zawawi, W.H. Azmi, A.A.M. Redhwan, M.Z. Sharif, Coefficient of friction and wear rate effects of different composite nanolubricant concentrations on Aluminium 2024 plate, in: *IOP Conference Series: Materials Science and Engineering*, vol. 257, 2017.
- [30] N.N.M. Zawawi, W.H. Azmi, A.A.M. Redhwan, M.Z. Sharif, Thermo-physical properties of metal oxides composite Nanolubricants, *J. Mech. Eng.* 15 (2018) 28–38.
- [31] M.Z. Sharif, W.H. Azmi, N.N.M. Zawawi, M.F. Ghazali, Comparative air conditioning performance using SiO₂ and Al₂O₃ nanolubricants operating with Hydrofluoroolefin-1234yf refrigerant, *Appl. Therm. Eng.* 205 (2022), 118053.
- [32] N.N.M. Zawawi, W.H. Azmi, M.F. Ghazali, Performance of Al₂O₃-SiO₂/PAG composite nanolubricants in automotive air-conditioning system, *Appl. Therm. Eng.* 204 (2022), 117998.
- [33] S. Aldrich, Safety data sheet, in: *Silicon Dioxide and Titanium Dioxide*, 2013.
- [34] W.H. Azmi, K.V. Sharma, P.K. Sarma, R. Mamat, G. Najafi, Heat transfer and friction factor of water based TiO₂ and SiO₂ nanofluids under turbulent flow in a tube, *Int. Commun. Heat Mass Tran.* 59 (2014) 30–38.
- [35] Emkarate, RL68H, in: *Typical Properties Data Sheet*, Lubrizol, CPI Engineering Services, 2016.
- [36] A. Asadi, I.M. Alarifi, V. Ali, H.M. Nguyen, An experimental investigation on the effects of ultrasonication time on stability and thermal conductivity of MWCNT-water nanofluid: finding the optimum ultrasonication time, *Ultrason. Sonochem.* 58 (2019), 104639.
- [37] ASHRAE, Standard, ASHRAE 41 (2011) 9–2000.
- [38] SAEJ2765, SAEJ2765-Procedure for Measuring System COP [Coefficient of Performance] of a Mobile Air Conditioning System on a Test Bench, SAE international, 2008, p. 20.
- [39] J.H. Lee, K.S. Hwang, S.P. Jang, B.H. Lee, J.H. Kim, S.U.S. Choi, C.J. Choi, Effective viscosities and thermal conductivities of aqueous nanofluids containing low volume concentrations of Al₂O₃ nanoparticles, *Int. J. Heat Mass Tran.* 51 (2008) 2651–2656.
- [40] T.M. Yusoff, A.R. Yusoff, Analysis for optimum refrigerant charge of a mini bar refrigerator using experimental method, *J. Eng. Technol.* 4 (2011) 1–12.
- [41] M.Z. Sharif, W.H. Azmi, A.A.M. Redhwan, R. Mamat, T.M. Yusoff, Performance analysis of SiO₂/PAG nanolubricant in automotive air conditioning system, *Int. J. Refrig.* 75 (2017) 204–216.
- [42] Z. Li, K. Liang, H. Jiang, Experimental study of R1234yf as a drop-in replacement for R134a in an oil-free refrigeration system, *Appl. Therm. Eng.* 153 (2019) 646–654.
- [43] F. Illán-Gómez, J.R. García-Cascales, Experimental comparison of an air-to-water refrigeration system working with R134a and R1234yf, *Int. J. Refrig.* 97 (2019) 124–131.
- [44] G. Yıldız, Ü. Ağbulut, A.E. Gürel, A review of stability, thermophysical properties and impact of using nanofluids on the performance of refrigeration systems, *Int. J. Refrig.* 129 (2021) 342–364.
- [45] H. Xie, B. Jiang, J. He, X. Xia, F. Pan, Lubrication performance of MoS₂ and SiO₂ nanoparticles as lubricant additives in magnesium alloy-steel contacts, *Tribol. Int.* 93 (2016) 63–70.
- [46] M.K.A. Ali, H. Xianjun, L. Mai, C. Bicheng, R.F. Turkson, C. Qingping, Reducing frictional power losses and improving the scuffing resistance in automotive engines using hybrid nanomaterials as nano-lubricant additives, *Wear* 364 (2016) 270–281.
- [47] M.Z. Sharif, W.H. Azmi, A.A.M. Redhwan, R. Mamat, Investigation of thermal conductivity and viscosity of Al₂O₃/PAG nanolubricant for application in automotive air conditioning system, *Int. J. Refrig.* 70 (2016) 93–102.
- [48] J. Wang, H. Xie, Z. Guo, L. Guan, Y. Li, Improved thermal properties of paraffin wax by the addition of TiO₂ nanoparticles, *Appl. Therm. Eng.* 73 (2014) 1541–1547.
- [49] F. Meng, M. Elshahati, J. Liu, R.F. Richards, Thermal resistance between amorphous silica nanoparticles, *J. Appl. Phys.* 121 (2017), 194302.